MEASURING AND MONITORING NEAR-SURFACE SHEAR WAVE VELOCITY AND ATTENUATION AT GARNER VALLEY

Lei Qin[1,2], Jamison H. Steidl[3], Kenneth S. Hudson[4], Timothy Lamere[5], Hongrui Qiu[6,7], Yehuda Ben-Zion[8]

[1]Department of Earth Sciences, University of Southern California, Los Angeles, CA, US
[2]Hubei Subsurface Multi-Scale Imaging Key Laboratory, Institute of Geophysics and Geomatics, China University of Geosciences, Wuhan, China
[3]Earth Science Institute, University of California, Santa Barbara, CA, US
[4]Civil and Environmental Engineering, University of California, Los Angeles, CA, US
[5]Manufacturing Design Engineer, Apple Inc.
[6]Department of Earth, Environmental and Planetary Sciences, Rice University, Houston, TX, USA
[7]Earth, Atmospheric and Planetary Sciences, Massachusetts Institute of Technology, Cambridge, MA, USA
[8]Southern California Earthquake Center, University of Southern California, Los Angeles, CA, USA

1. Key points

- **Average in the top 6 m: Impulse response functions (IRFs) at 6-22 m; Vs ~200 m/s, with ~10% seasonal variation**
- **At 5 m depth: Cross-hole array experiment; Vs ~ 210-227 m/s, with ~6% seasonal variation; frequency-dependent Q values are less than 10.**
- **Vs decreases with the precipitation (i.e. water table) and temperature with a phase delay of ~64 days.**
- **S-wave velocity variations decrease with depth**
- **Possible structure variation induced by thermoelastic strains in the top ~1 m**

2. Data – Garner Valley Downhole Array (GVDA)

Figure 1. Event and Array information

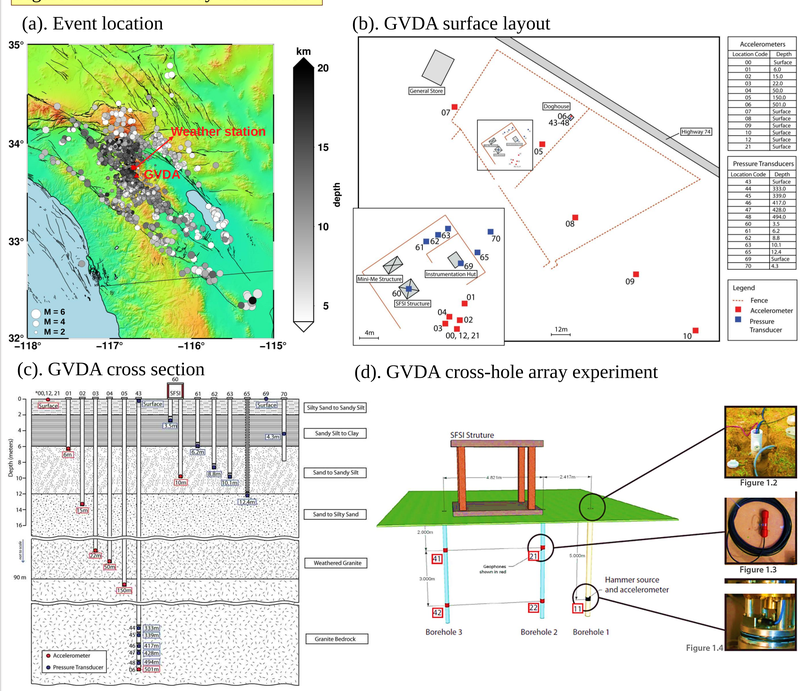

Figure 1. (a). Events (circles) with high-quality (SNR>2) S-wave arrivals at GVDA (red triangle) from 2005 to 2021. The red square shows the location of the Idyllwild weather station that is used in this study. (b) Surface layout of the GVDA, with accelerometers (red squares) and pore pressure transducers (blue squares). (c) Conceptual cross-section placement of the GVDA, showing seismic stations (red dots) at 0-501 m and pore pressure sensors (blue dots) at 0-12.4 m. (d). Cross-hole array experiment at GVDA, with a solenoid powered, dual directional hammer located at 5 m in depth and four geophones, two located at 5 m (22, 42) and the other two (21, 41) directly above them at 2 m in depth. An accelerometer (11) is also mounted to the hammer strike plate. The sampling rate of the geophones is 2000 samples per second. (b)(c)(d) are available from http://nees.ucsb.edu/facilities/GVDA.

Figure 2. Cross-hole array experiment data

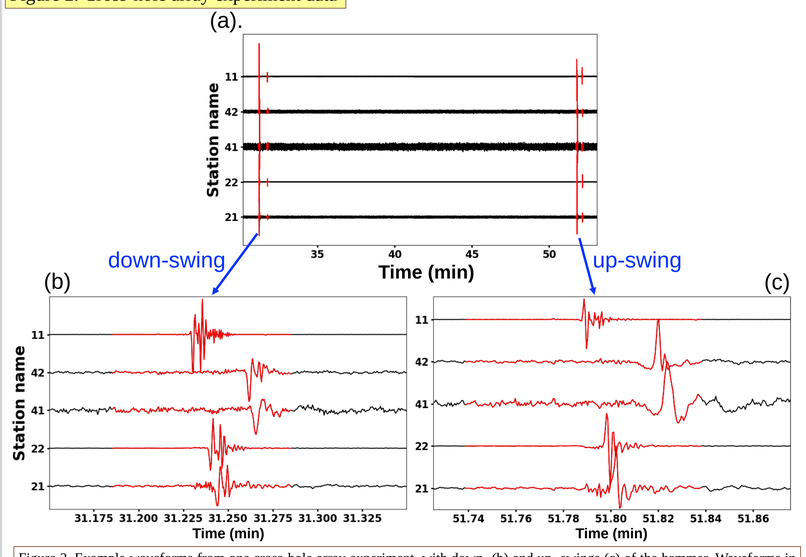

Figure 2. Example waveforms from one cross-hole array experiment, with down- (b) and up- swings (c) of the hammer. Waveforms in red (6 sec centered at the location of the maximum amplitude in station 11) are later analyzed for the S-wave delay time and frequency-dependent Q values between stations. For illustration purpose, the amplitude information is not preserved in the figure.

3. Impulse response functions (IRFs) analysis

Figure 3. IRF examples

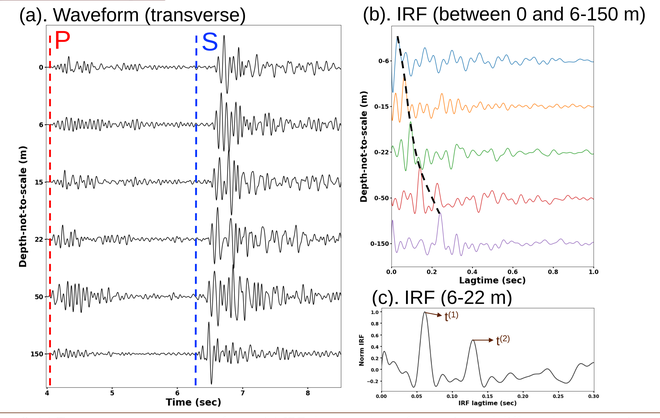

Figure 3. (a) Transverse-component waveforms. (b) IRFs between the surface station and different borehole stations, calculated in the time window 1 sec before and 5 sec after the S-wave arrival. Black dashed line connects the primary peak representing the travel time from surface to borehole stations. (c) IRF between the 6 m (01) and 22 m (03) borehole stations. The primary peak at $t^{(1)}$ (~0.065 sec) represents SH-wave travel time from 22 m to 6 m, and the secondary peak at $t^{(2)}$ (~0.125 sec) shows the travel time from 22 m to the 6 m borehole which is reflected at the free surface.

Figure 4. IRF results 1-30 Hz IRF; 01 (6 m)-03 (22 m); transverse component)

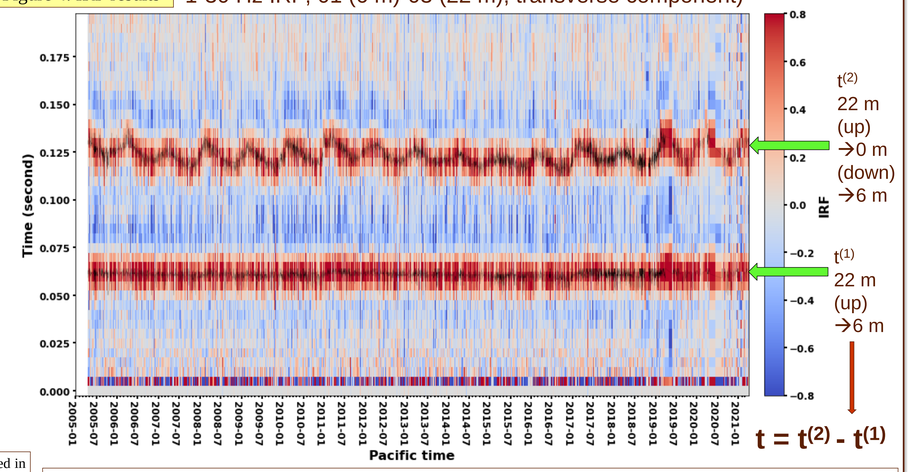

Figure 4. SH-wave IRFs between the 6 m (01) and 22 m (03) borehole stations (similar to Fig. 3c). Waveforms are band pass filtered at 1-30 Hz and each IRF is normalized by the maximum amplitude. Horizontal axis shows the event occurrence time and vertical axis is the IRF lagtime. The change of $t=t^{(2)}-t^{(1)}$ represents the temporal change of the material in the top 6 m.

Figure 5. dt/t vs. precipitation

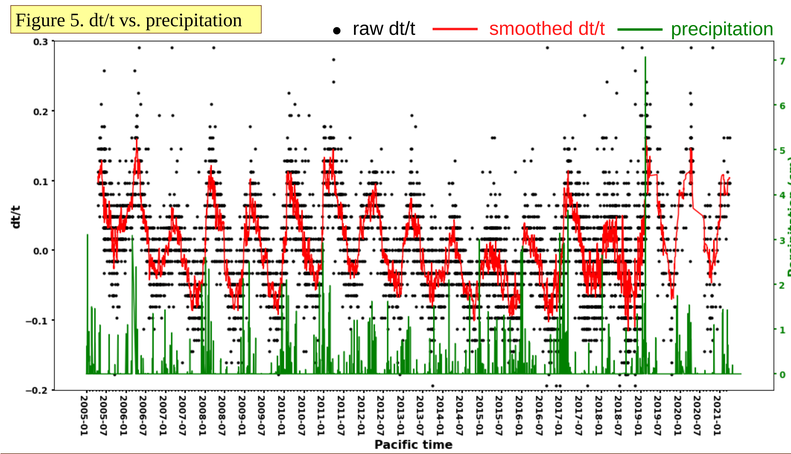

Figure 5. Comparison between the travel time variation (dt/t; black dots and red curve) and the precipitation data (green curve) from the Idyllwild weather station. Here $dt/t=(t-t_0)/t_0$, where t_0 is the median value of all the t measurements (black dots). The red curve is the 11-point smoothed dt/t .

Figure 6. dt/t vs. temperature

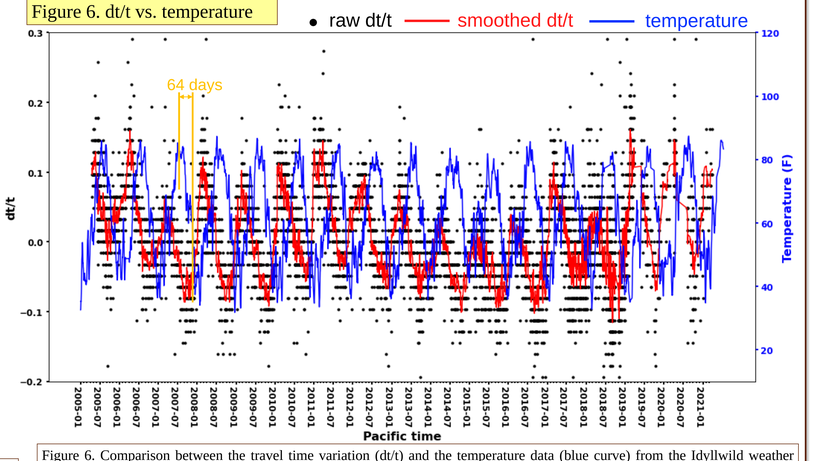

Figure 6. Comparison between the travel time variation (dt/t) and the temperature data (blue curve) from the Idyllwild weather station. Here the black dots and red curve are the same as in Fig. 5. The apparent phase delay of -dt/t (i.e. dv/v) curve relative to the temperature is ~64 days.

4. Cross-hole array experiment

Figure 7. Q value estimation

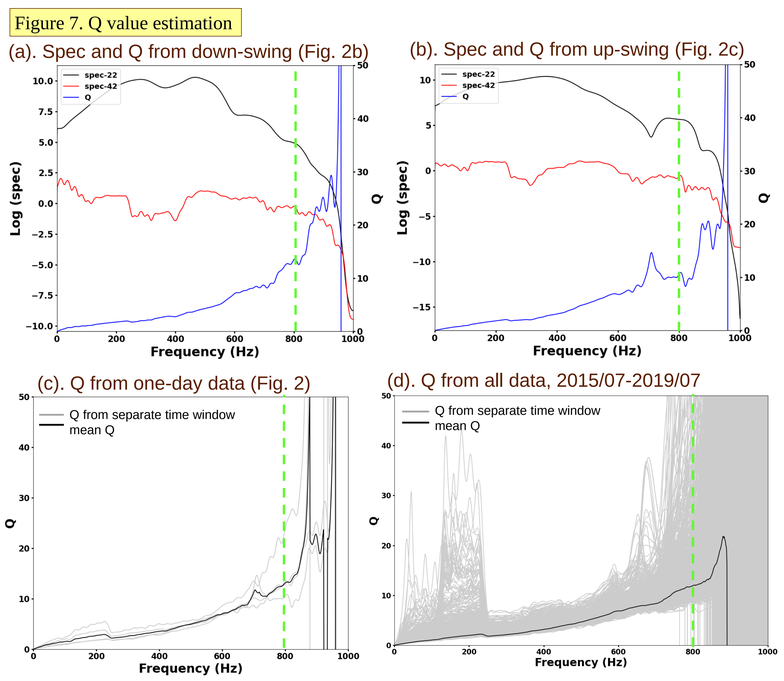

Figure 7. (a) Power spectral density of down-swing data (Fig. 2b) at station 22 (black curve) and 42 (red curve), and the corresponding frequency-dependent Q values (blue curve). The results are reliable up to 800 Hz (green dashed line). (b) same as (a), but for up-swing data (Fig. 2c). (c) Frequency-dependent Q values (gray curves) from the four time windows in one-day data (in red in Fig. 2a), and the corresponding median value (black curve). (d) All Q values from cross-hole array experiment data (gray curve) and the corresponding median values (black curve).

Figure 8. S-wave travel times between stations 42 and 22 obtained via cross-correlation

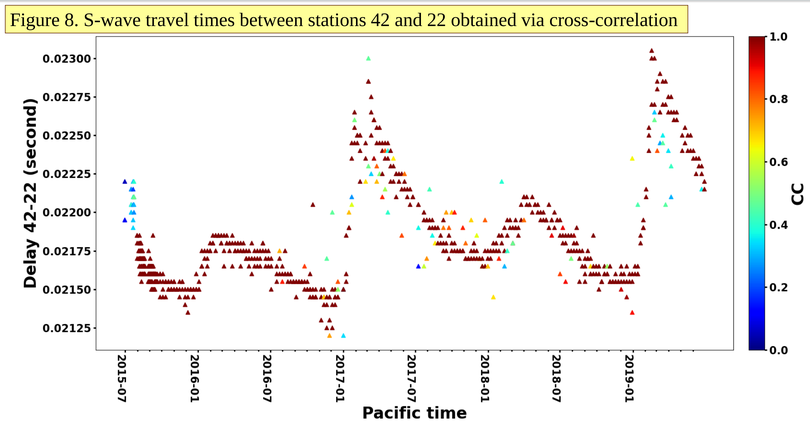

Figure 9. Comparison of dt/t in the top 6 m (red curve) and at the 5 m depth (black triangles).